Desalination and Water Treatment
www.deswater.com

doi: 10.5004/dwt.2019.23609

145 (2019) 369–377
March

Xylenol orange removal from aqueous solution by natural bauxite (BXT) and BXT-HDTMA: kinetic, thermodynamic and isotherm modeling

Muna A. Al-Kazragi, Dhafir T.A. Al-Heetimi*, Omar S.A. Al-Khazrajy

[a]*Department of Chemistry, College of Education for Pure Science Ibn Al-Haitham, University of Baghdad, Baghdad, Iraq, Tel. +964-790-217-7896, email: Muna.rasool@yahoo.com (M.A. Al-Kazragi), Tel. +964-770-882-6565, email: dhafir1973@gmail.com, dhafir73@yahoo.com, dhafir.t.a@ihcoedu.uobaghdad.edu.iq (D.T.A. Al-Heetimi), Tel. +964-771-557-4914, email: omar.s.a@ ihcoedu.uobaghdad.edu.iq (O.S.A. Al-Khazrajy)*

Received 1 April 2018; Accepted 12 December 2018

ABSTRACT

Sorption is a key factor in removal of organic and inorganic contaminants from their aqueous solutions. In this study, we investigated the removal of Xylenol Orange tetrasodium salt (XOTS) from its aqueous solution by Bauxite (BXT) and cationic surfactant hexadecyltrimethyl ammonium bromide modified Bauxite (BXT-HDTMA) in batch experiments. The BXT and BXT-HDTMA were characterized using FTIR, and SEM techniques. Adsorption studies were performed at various parameters i.e. temperature, contact time, adsorbent weight, and pH. The modified BXT showed better maximum removal efficiency (98.6% at pH = 9.03) compared to natural Bauxite (75% at pH 2.27), suggesting that BXT-HDTMA is an excellent adsorbent for the removal of XOTS from water. The equilibrium data of XOTS adsorption on BXT and BXT-HDTMA surfaces were best fitted with the Freundlich isotherm model. The pseudo-second-order model provided very good fitting for the dye on the two surfaces. The error function, the sum of the absolute errors (SAE), was calculated to identify the best isotherm in this study. The thermodynamic parameters like ΔH^o, ΔS^o and ΔG^o were also calculated. The adsorbent dosage weight and pH were found the most factors influencing the removal process.

Keywords: Anionic dye; Cationic surfactant; Iraqi Bauxite mineral clay; Thermodynamic parameters

1. Introduction

Concerns over the occurrence of organic and inorganic pollutants in the aquatic environment has recently increased [1]. Industrial wastewater discharges (e.g. textiles, food, plastics, paper-making, rubber and cosmetics) were found to be one of the main sources of organic pollutants which may consequently reach aquatic environment and affect the water quality [2–4]. One of the widely detected chemicals is industrial dyes. This kind of chemicals are persistent organic pollutants (POPs) and have been found to have high photostability and resistance to biodegradation and oxidation agents during wastewater treatment processes [5,6]. It was found that even at low concentration in water, dyes cab be accumulated in the aquatic environment and threat both humans and environmental organisms through promoting carcinogenic activity, teratogenicity, chromosomal fractures and respiratory toxicity [5]. XOTS is an anionic dye causes skin and eye irritation, gastrointestinal irritation with vomiting, nausea and diarrhea [7]. Some physical and chemical methods including coagulation, separation, chemical oxidation, electrochemical processes, membrane, and adsorption process have been used for dyes removal from aquatic environment [3,8–10]. Some of those methods have proven to be either too expensive or inefficient to remove contaminants from water [1]. Among these removal methods, adsorption process is more advantageous due to high treatment efficiency. Moreover, many adsorbents tested such as activated carbon [11], kaolin [12], bentonite [13] and zeolite [14] are naturally existed and available at low cost. Recently, adsorption of organic chemicals on metal (e.g. Al^{+3}, Mg^{+2}) hydroxides using electrochemical coagulation has been investigated and showed a high removal efficiency of up to 91.0% [6].

*Corresponding author.

Several studies on XOTS adsorption from aqueous solutions were carried out. Jugal et al. studied adsorption of XOTS by two types of low-cost adsorbent were prepared from fruits of Kigelia Africana (KA) and Melia Azedarach (MA) trees. Experimental results indicate that (KA) and (MA) fruits based adsorbents have significant effect for XOTS removal from its aqueous solutions [15]. Chen et al. [16] studied the removal of XOTS from aqueous solution based on Chromium-Benzene di carboxylates. The adsorption isotherm and kinetic agreed with the Langmuir isotherm and pseudo-second-order. Iraqi Bauxite (BXT) is a hard-solid mineral clay with high porosity. BXT surface consists mainly of aluminum hydroxide and silica. Generally, Bauxite consist from mixed heterogeneous minerals such as Gibbsite, Boehmite, kaolinite and Diaspore with small quantities of impurities like (Fe_2O_3, TiO_2, CaO, MgO, Na_2O and K_2O) [17].

For the present study, the objectives were to 1) study the effect of using organic modifier (HDTMA, cationic surfactant) on adsorption capacity of BXT for the removal of XOTS; 2) study the effect of adsorbent weight and pH on the removal of XOTS; 3) study the adsorption isotherms using Langmuir, Freundlich and Temkin models; 4) investigate the adsorption kinetics of XOTS from aqueous solutions; and 5) calculate the thermodynamic parameters for the adsorption of XOTS at different temperatures.

2. Material and experiment methods

2.1. Material

The anionic dye used in this work was Xylenol Orange tetrasodium salt (XOTS) $C_{31}H_{28}N_2Na_4O_{13}S$. The dye (90%) was used without any further purification and the surfactant hexadecyltrimethyl ammonium bromide (HDTMA) ≥99% was purchased from Sigma-Aldrich. Bauxite mineral clay was supplied from the general company for Geological Survey and Mining, Baghdad, Iraq. The chemical analysis of BXT (Al_2O_3 50.64, SiO_2 31.03, Fe_2O_3 2.75, CaO 0.04, MgO <0.02, Na_2O 0.02, TiO_2 1.80, K_2O 0.02, L.O.I 13.0, Total = 99.82%).

2.2. Preparation of organoclay

BXT was washed and dried at a temperature of (90°C) for 6 h, cooled at room temperature, and after that kept in airtight container. The mineral clay was ground and sieved to (≤ 75 µm sample) by using sieve (200 mesh). The adsorbent was modified to organocaly by treating the BXT with HDTMA surfactant. For the preparation, 3.5 g of HDTMA was dissolved in 1 L of deionized water and then added to (50 g) of BXT. The suspension was stirred for 24 h at room temperature, decanted, washed several times with deionized water and then dried at 90ºC for 6 h. The adsorbent obtained was ground in powder form and sieved to get (≤75 µm sample).

2.3. Characterization of the modified adsorbent

The Fourier transforms infrared spectroscopy (FTIR) (Shimadzu 8400, Japan) in the wavenumber range from (4000–400 cm^{-1}). The adsorbent surface morphology of BXT and modified adsorbent (BXT-HDTMA) surfaces were characterized using scanning electron microscope (SEM) type - TE-Scan (Vega-11, Czech Republic).

2.4. Adsorption experiments

Adsorption isotherms of XOTS onto BXT and BXT-HDTMA were investigated at different concentrations ranging from 10–70 mg/L. Briefly, 0.2 and 0.1 g of BXT and BXT-HDTMA surfaces were placed separately in a screw cap bottle, and 10 mL of serial XOTS solution was added to each bottle (three replicates) and placed in thermos stated shaker at various temperature (25, 35 and 45°C). The shaking was continued for a period exceeding the time to reach equilibrium for the adsorbents surfaces. At the end of the adsorption period, the samples were removed and transferred to be centrifuged (Hettich EBA-20, Germany, 6000 rpm) at 2500 rpm for 10 min. Supernatant were then filtered using filter paper (Whitman No. 42) prior to analysis. The clear supernatants were assayed spectrophotometrically for XOTS using UV-VIS spectrophotometer double beam type T-80 England. The UV-Visible spectrophotometer, double beam (T80, USA) scanning spectra has been recorded and wavelength value was found to be (580 nm). The adsorption capacity of BXT and BXT-HDTMA was calculated according to Eq. (1):

$$q_e = \frac{X}{m} = \frac{(C_o - C_e) \times V}{W} \quad (1)$$

where C_o is the initial XOTS concentration and C_e is the equilibrium XOTS concentration in mg/L; while q_e is the amount of anionic dye adsorbed after equilibrium in mg/g. (V) is the sample volume (L) and W is the weight of the adsorbent (g).

The XOTS removal percentage (R%) was determined from the relationship:

$$R\% = \frac{C_o - C_e}{C_o} \times 100 \quad (2)$$

3. Results and discussion

3.1. FTIR spectra

FTIR spectra of natural Bauxite (BXT) and modified Bauxite (BXT-HDTMA) surfaces were measured as shown in Figs. 1a, b. The bands in Fig. 1a at 3691 and 3618 cm^{-1} related to the OH stretching vibrations of the hydroxyl group. The two bands at 914 and 738 cm^{-1} are assigned to Al-O-Al and Si-O-Si groups respectively, while the band at 1033 cm^{-1} is assigned to Si-O group. After modification with surfactant HDTMA (Fig. 1b), the bands at 3618, 1033 and 738 cm^{-1} shifted and changed the intensity of these bands. Modified Bauxite shows peaks at 2920 and 2850 cm^{-1} which related to the symmetric and asymmetric stretching vibrations of methyl (–CH_3) and methylene (–CH_2) groups of the cationic surfactant [18].

3.2. SEM characterization

The scanning electron microscopic photographs illustrate the crystalline structure, surface porosity and texture

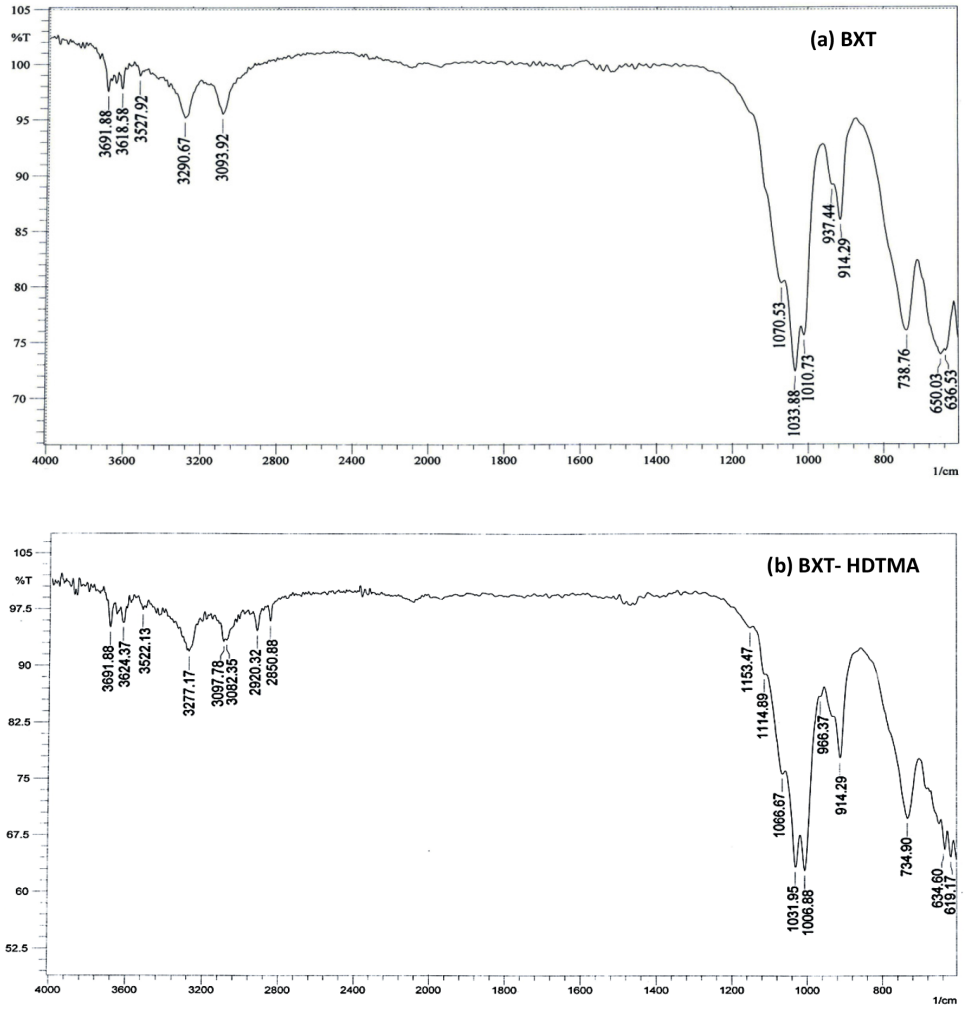

Fig. 1. FTIR spectra of (a) BXT and (b) BXT-HDTMA.

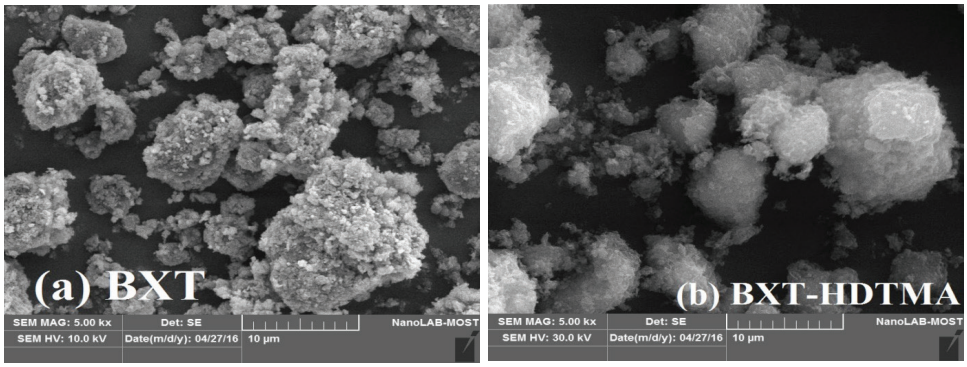

Fig. 2. (a) SEM photograph of BXT surface (b) SEM photograph of BXT-HDTMA surface.

of surface materials. The SEM photographs of BXT and BXT-HDTMA surfaces are reported in Figs. 2a, b. The photograph (Fig. 2a) shows the smooth and flat crystal surface of the BXT. On the other hand, when the surface was modified with HDTMA, the BXT lattice appeared swollen and fluffy; because of an increasing in interparticle spacing of BXT surface [19]. These changes is clearly shown in Fig. 2b.

3.3. Effect of adsorbent weight

The effect of adsorbent weight to remove anionic dye by BXT and BXT-HDTMA surfaces is shown in Fig. 3. The removal of XOTS was analyzed at initial concentration of C_o = 30 mg/L onto BXT and BXT-HDTMA surfaces at 25°C. The removal percentage of pollutant by BXT declined with

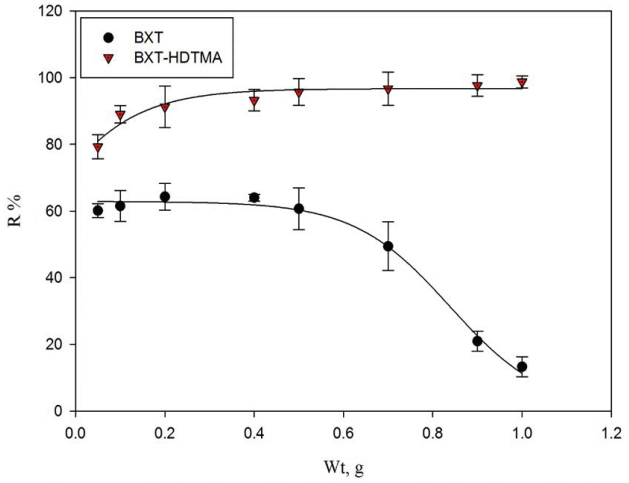

Fig. 3. The effect of adsorbent surface weight on the removal of XOTS onto BXT and BXT-HDTMA at 25°C and pH 6.54.

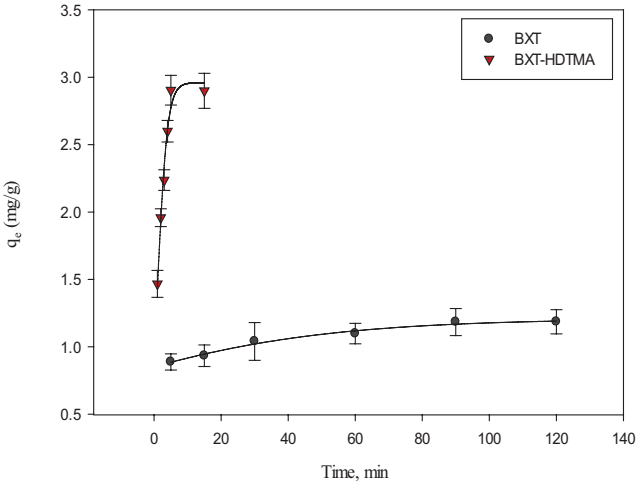

Fig. 4. The effect of contact time on XOTS adsorption onto BXT and BXT-HDTMA at 25°C and pH 6.54.

the increasing of adsorbent weight due to an increase of unsaturated adsorption sites [20]. However, the R% of dye onto BXT-HDTMA surface increased with increasing adsorbent weight. These results indicate that the formation of BXT-HDTMA (after surfactant modification) increase the removal of XOTS. This increase in removal is related to the change of hydrophobicity of the adsorbent and/or the increase of the BXT surface area which offers more vacant surface sites [3].

3.4. Effect of contact time

The adsorption of XOTS onto BXT and BXT-HDTMA surfaces was tested at initial XOTS concentration of (35 mg/L). The temperature and pH were affixed at 25°C and 6.54. Fig. 4 shows that the adsorption capacity of XOTS increases with time and reaches a constant value at a certain time. The equilibrium time was found to be 120 min for BXT and 30 min for BXT-HDTMA. It is evident that the adsorption capacity of BXT surface and BXT-HDTMA surface increased rapidly by the increase of contact time due to the availability of vacant sites on two surfaces [21].

3.5. Effect of pH

The pH effect on the adsorption of XOTS onto BXT and BXT-HDTMA surfaces was investigated at 25°C, initial concentration of 35 mg/L and adsorbent weight of 0.2 and 0.1 g, respectively. To obtain the desired pH a few drops of 0.1 M NaOH and HCl was added. Fig. 5 shows that the removal percentage of XOTS onto BXT surface increases with decreasing pH whereas, the R% of dye decreases with decreasing pH for BXT-HDTMA surface. For BXT surface, at low pH values, BXT surface consists of (Al and Si) metal oxides. These oxides tend to form complexes of metal-hydroxide in its aqueous solution to result a positively charged surface as shown in mechanism below where (M = Al, Si). Then attraction forces

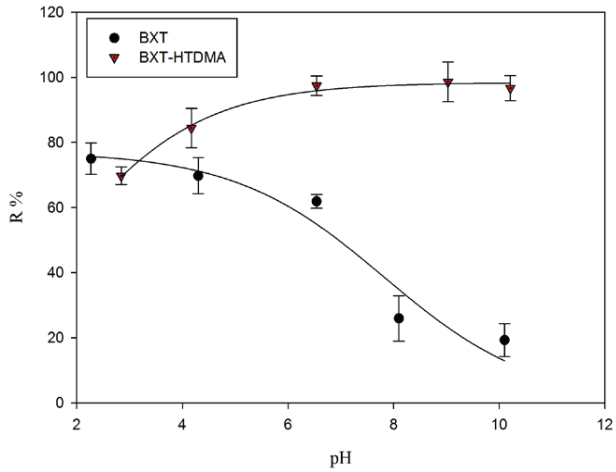

Fig. 5. Effect of pH solution on the removal of XOTS onto BXT and BXT-HDTMA surfaces at 25°C.

occur between the XOTS and the positively charged adsorbent surface [22].

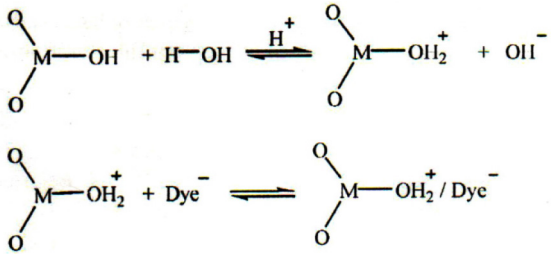

For BXT-HDTMA surface, at low pH solution, the sulphonate ($-SO_3^-$) groups of anionic dye may be protonated ($-SO_3H$, i.e., neutral). Moreover, the nitrogen atoms were probably protonated, thus the dye molecules will be either partially positively charged or neutral and the adsorbent surface is positively charged. Therefore, large

reduction in dye adsorption capacity can be related to repulsion forces between the BXT-HDTMA and the protonated XOTS dye [23].

3.6. Isotherm modeling

Three adsorption isotherm models were used to identify the mechanism of XOTS adsorption process on BXT and BXT-HDTMA. It is important to establish the most appropriate correlation for the equilibrium curves. The equilibrium data were generally examined using Langmuir, Freundlich and Temkin models [24–27]. The linearized Langmuir model, which is quantitatively describes the formation of monolayer chemosorption on the homogenized surface of the adsorbent, is presented as in Eq. (3):

$$\frac{C_e}{q_e} = \frac{1}{K_L q_m} + \frac{C_e}{q_m} \tag{3}$$

The Freundlich adsorption isotherm, which is typically indicate the heterogeneity of the adsorbent surface and the possibility of the formation of more than adsorbate layer on the surface [7] is presented in linear form as follows:

$$\log q_e = \log K_f + \frac{1}{n}\log C_e \tag{4}$$

The Temkin isotherm, which assumes that heat of adsorption (function of temperature) of all molecules in the layer would decrease linearly rather than logarithmic with coverage [27], the model is given by the following Eq. (5):

$$q_e = BLnA_T + BLnC_e \tag{5}$$

where q_m (mg/g) is the maximum adsorption capacity and K_L (L/mg) is Langmuir constant. q_m and K_L values can be determined from the slope and intercept of the linear plots of C_e/q_e against C_e. K_F (mg/g) and n are Freundlich constants which are determined from the values of slope and intercept of the plots of log q_e against log C_e, the Temkin model constants, (A_T) is the equilibrium binding constant, and (B) is the Temkin constant being estimated from the slope and intercept of the plots of q_e against ln (C_e) [28].

From the values of R^2 given in Table 1, it appears that Freundlich isotherm was the better choice to describe the adsorption process. However, K_F and n are parameters characteristic of the sorbent-sorbate system, which must be determined by data fitting and whereas linear regression is generally used to determine the parameters of kinetic and isotherm models [27]. Since the n value is greater than 1 (it has been reported that values of n lying between 0 and 10) indicate favorable adsorption [1] for BXT and BXT-HDTMA, cooperative adsorption is expected and more favorable to BXT-HDTMA than BXT.

3.7. Thermodynamic analysis

Thermodynamic parameters like the standard enthalpy change (ΔH°), standard entropy change (ΔS°) and standard free energy (ΔG°) for the adsorption of XOTS with BXT and BXT-HDTMA are estimated by using the Eqns. (6) and (8) at different temperatures (298 K, 308 K and 318 K) [29]:

$$\Delta G^\circ = -RT \ln K^o \tag{6}$$

where R is the gas constant (8.314J·mol^{-1} K^{-1}) and T is the absolute temperature.

The distribution adsorption coefficient (K_d) [30] is determined by the following equation

$$K_d = \frac{C_o - C_e}{C_e} \times \frac{V}{W} \tag{7}$$

where C_o is the initial XOTS concentration and C_e is the equilibrium XOTS concentration in (mg/L). (V) is the sample volume (mL) and W is the weight of the adsorbent (g).

The standard enthalpy change (ΔH°) and the standard entropy change (ΔS°) were determined using Eq. (8):

$$\ln K^o = \Delta S^\circ/R - \Delta H^\circ/RT \tag{8}$$

The equilibrium constant (K^o) was determined by plotting ln K_d against C_e and extrapolating C_e to 0. The value of the intercept is that of ln K^o. The values of ΔG° were estimated from Eq. (6) at constant temperature. Values of ΔH° and ΔS° were calculated by plotting ln K^o against 1/T. For both systems (BXT and BXT-HDTMA), the negative ΔG° val-

Table 1
Isotherm parameters for XOTS adsorption onto BXT and BXT-HDTMA surfaces

Isotherm	Adsorbent	298 K			308 K			318 K		
		K_L (L/mg)	q_{max} (mg/g)	R^2	K_L (L/mg)	q_{max} (mg/g)	R^2	K_L (L/mg)	q_{max} (mg/g)	R^2
Langmuir	BXT	0.0542	2.7397	0.9314	0.0538	2.3201	0.9422	0.0531	2.1008	0.9609
	BXT-HDTMA	0.0787	5.3763	0.9729	0.1321	5.1813	0.9694	0.2045	5.1020	0.9757
Freundlich		K_F (mg/g)	$1/n$	R^2	K_F (mg/g)	$1/n$	R^2	K_F (mg/g)	$1/n$	R^2
	BXT	0.2382	0.585	0.9810	0.2123	0.564	0.9920	0.1967	0.552	0.9978
	BXT-HDTMA	0.6151	0.554	0.9970	0.9183	0.469	0.9942	1.2022	0.416	0.9904
Temkin		B	A_T	R^2	B	A_T	R^2	B	A_T	R^2
	BXT	0.541	0.6561	0.9322	0.477	0.6033	0.9405	0.438	0.5794	0.9518
	BXT-HDTMA	1.112	0.8802	0.9588	1.023	1.6951	0.9451	0.954	3.1018	0.9467

ues (–12.23, –12.17 and –12.20 kJ/mol), (–14.70, –16.35 and –17.90 kJ/mol) at 298, 308 and 318 K, respectively, indicate that the adsorption process of anionic dye is spontaneous [10,31]. The value of ΔH° (–12.65 kJ/mol) indicate that the adsorption of XOTS onto BXT is exothermic in nature, while ΔH° value of 33.2 kJ/mol suggesting that the adsorption of dye by BXT-HDTMA surface is endothermic [32,33]. The negative value of ΔS° (–1.48 J/mol·K) for anionic dye onto BXT surface suggesting that randomness decreases during adsorption [34]. On the other hand, the positive value of ΔS° (160.13 J/mol·K) for XOTS onto BXT-HDTMA surface indicates that random increase during adsorption [35].

3.8. XOTS kinetic study

To explain the removal of XOTS process on the adsorbents, the order and the rate constant were evaluated using kinetic data. The experimental kinetic data were tested using two models pseudo-first order (PFO) [Eq. (9)] and pseudo-second order (PSO) [Eq. (10)] to evaluate the mechanism involved in the XOTS adsorption process at concentration of 35 mg/L.

$$Ln(q_e - q_t) = Lnq_e - k_1 t \tag{9}$$

$$\frac{t}{q_t} = \frac{1}{k_2 q_e^2} + \frac{1}{q_e} t \tag{10}$$

where k_1 (min^{-1}) and k_2 (g·mg^{-1}·min^{-1}) are the rate constants, respectively [36], q_e and q_t (mg/g) are the concentrations of the XOTS adsorbed at equilibrium and any contact time of adsorption t (min), respectively. The experimental data were analyzed initially with pseudo first order model. The PFO constants (k_1 and q_e) were determined from slopes and intercepts as shown in Figs. 7a, b and Table 2. The PFO model gives poor suitable with low R^2 values and the calculated q_e value does not agree to the experimental q_e at concentration of 35 mg/g [37]. Therefore, PSO is more suitable model to describe the experimental kinetic data of XOTS adsorption process by BXT and BXT-HDTMA surfaces [6,38]. PSO constants k_2 and q_e were determined from the slopes and intercepts from Fig. 8a, b, respectively. PSO were found to be linear and showed good fitting with R^2 greater than 0.9715. The calculated q_e values (Table 2) agreed well with the experimental q_e values at all temperatures studied. This implies that the PSO model is in good agreement with experimental data and can be used to favourably explain the XOTS adsorption on BXT and BXT-HDTMA.

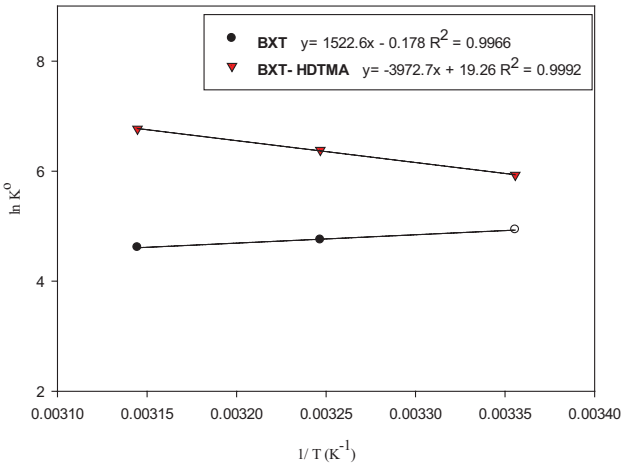

Fig. 6. The relationship of Ln K° versus 1/T.

3.9. Error analysis

In order to examine the goodness of fit for three isotherm models, error faction (SAE) was determined using Eq. (11) [39]:

$$SAE = \sum_{i=1}^{n} \left(\left| q_{e,calc} - q_{e.exp} \right| \right)_i \tag{11}$$

where $q_{e,exp}$ and $q_{e,calc}$ are the observation from the experiment and the estimate from the isotherm for corresponding $q_{e,exp}$,

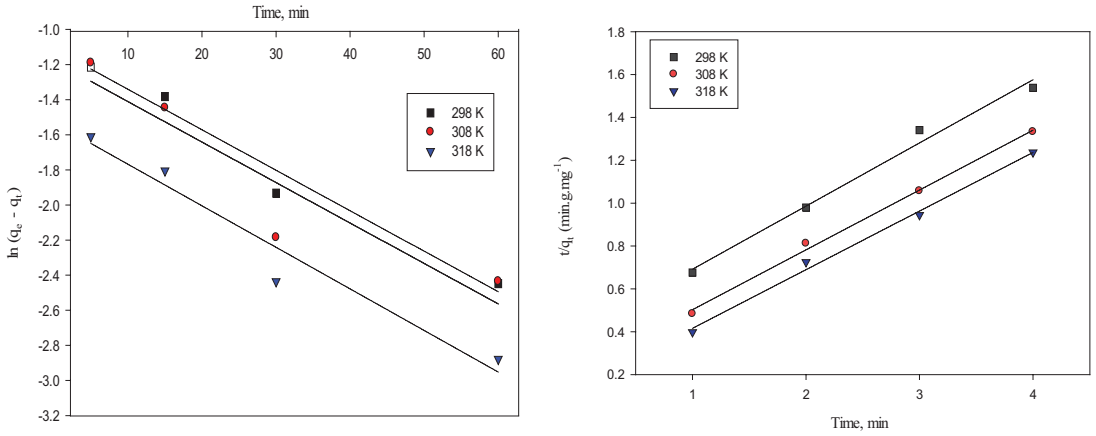

(a) (b)

Fig. 7. Pseudo-first order kinetics for XOTS dye adsorption onto (a) BXT and (b) BXT- HDTMA at different temperatures.

Table 2
Kinetics parameters for the adsorption of XOTS onto BXT and BXT-HDTMA surfaces (C_o = 35 mg/L)

Adsorbent	T(K)	Pseudo-first order				Pseudo-second order		
		K_1 (min^{-1})	$q_{e,exp}$ mg/g	$q_{e,calc}$ mg/g	R^2	K_2 (g·mg^{-1}·min^{-1})	$q_{e,calc}$ mg/g	R^2
BXT	298	0.0201	1.1833	0.3596	0.9250	0.3245	1.1025	0.9986
	308	0.0255	0.9895	0.3442	0.8571	0.3497	0.9514	0.9993
	318	0.0242	0.3729	0.2016	0.7904	0.4117	0.3595	0.9874
BXT-HDTMA	298	0.4605	2.3625	1.6372	0.9504	0.3840	2.5641	0.9830
	308	0.4969	2.6583	2.0875	0.9443	0.4942	3.0120	0.9715
	318	0.5280	2.7666	2.1043	0.9803	0.7032	3.1645	0.9878

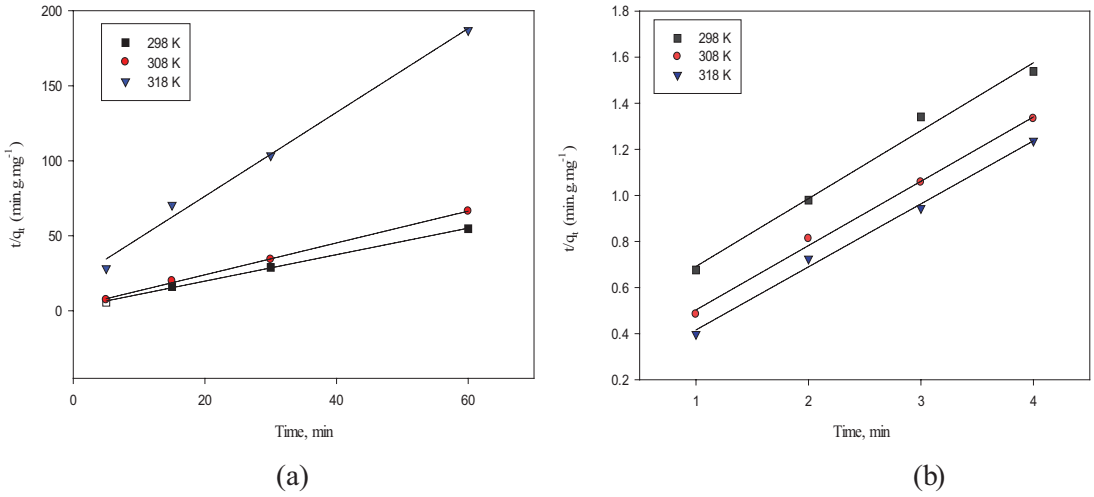

Fig. 8. Pseudo-second order kinetics for XOTS dye adsorption onto (a) BXT and (b) BXT- HDTMA at different temperatures.

respectively. The SAE parameters listed in Table 3 suggesting that Temkin isotherm provides a better model of the adsorption systems.

3.10. Removal efficiency and suggested adsorption mechanism

Based on the results obtained from the laboratory scale experiments, the best removal of XOTS on BXT and BXT-HDTMA was achieved. The BXT showed maximum removal efficiency of 75% at pH = 2.27 while BXT-HDTMA showed maximum removal (98%) at pH of 9.03. Moreover, adsorbent weight showed to be inversely correlated to the removal efficiency. The modified BXT showed better maximum removal efficiency (98.8% at dosage weight of 1.0 g compared to BXT which showed low removal efficiency of 13.5% at wt = 1.0 g. Generally, the results of this study showed better removal of XOTS on BXT-HDTMA in comparison to those reported in the literature. Shakeel et al. [40] developed and evaluated sodium dodecyl sulfate (SDS) self-microemulsifying systems (SMES) for the removal of XOTS from aqueous media via liquid–liquid adsorption with maximum removal of 89.77%. Chen et al. [16] used porous metal-organic framework (MOF) material based on chromium-benzenedicarboxylates for the adsorption of XOTS from aqueous solution with removal efficiency of 90%. Recently, coal ash as a low cost adsorbent was used for the removal of XOTS from aqueous solutions with removal efficiency of up to 80% [8]. These results suggesting that BXT-HDTMA is an excellent adsorbent for the removal of XOTS from aqueous solutions.

Table 3
Isotherm error analysis for adsorption XOTS onto BXT and BXT-HDTMA surfaces at different temperature

Adsorbent	Isotherm	T=298.15K	T=308.15 K	T=318.15K
BXT	Langmuir	0.0611	0.0527	0.0593
	Freundlich	0.0335	0.0325	0.0179
	Temkin	0.0129	0.0086	0.0145
BXT-HDTMA	Langmuir	0.1762	0.2280	0.2362
	Freundlich	0.0283	0.2795	0.2516
	Temkin	0.0048	0.0124	0.0138

According to the surface morphology of BXT and BXT-HDTMA and the nature of XOTS (anionic), we have tried to suggest the mechanism of interaction between the sorbents and the XOTS. Due to outer negative charge of XOTS and BXT, electrostatic repulsion is highly expected at neutral and basic pH, which explain the low adsorption capacity of BXT [41]. The negative charge is balanced by the presence of replaceable cations such as Ca^{2+} or Na^{+} in the lattice structure and the suggested adsorption mechanism is cationic bridging (Fig. 9).

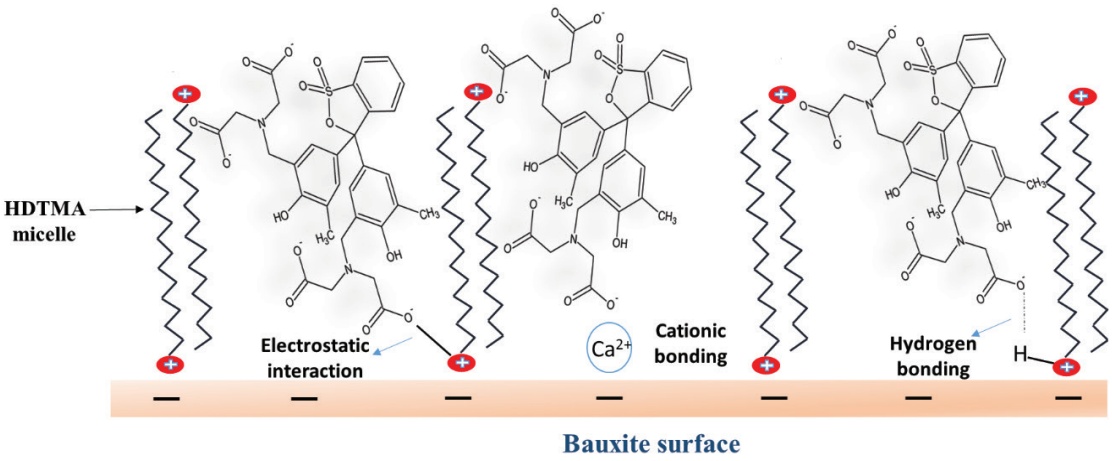

Fig. 9. Suggested interaction mechanisms of XOTS onto BXT and BXT-HTDMA.

In greater pH values, the ion exchange, H-bonding and water bridging are the potential mechanism of interaction [42]. On the other hand, the potential interaction between XOTS and BXT-HDTMA, the positive charge is dominant; it is expected to be via different mechanisms including electrostatic interaction to the positively charged head of HDTMA and hydrogen bonding to be responsible of the adsorption process [42] (Fig. 9).

4. Conclusion

We have successfully prepared and characterized HDTMA-modified Bauxite for the removal of XOTS dye from its aqueous solution. The adsorption capacities of modified BXT for XOTS were greater than those for BXT. The kinetic data fitted well to the pseudo-second order model. The adsorption of XOTS by BXT and BXT-HDTMA surfaces were successfully described by Freundlich isotherm. Thermodynamic analysis indicated that adsorption of XOTS onto BXT and BXT-HDTMA surfaces was thermodynamically feasible, spontaneous, exothermic in nature for removal of XOTS dye by BXT surface and endothermic for removal of XOTS by BXT-HDTMA surface. The results from this work suggest that BXT-HDTMA is suitable for removal of XOTS from its aqueous solutions.

Acknowledgment

The authors would like to thank the Chemistry department, College of Education for pure science Ibn Al-Haitham for facilitating this research work.

References

[1] R. Kamaraj, S. Vasudevan, Facile one-pot synthesis of nano-zinc hydroxide by electro-dissolution of zinc as a sacrificial anode and the application for adsorption of Th^{4+}, U^{4+}, and Ce^{4+} from aqueous solution, Res. Chem. Intermed., 42 (2016) 4077–4095.
[2] T.S. Anirudhan, M. Ramachandran, Adsorptive removal of basic dyes from aqueous solutions by surfactant modified bentonite clay (organoclay): kinetic and competitive adsorption isotherm, Process Saf. Environ. Prot., 95 (2015) 215–225.
[3] L.G. Yan, L.L. Qin, H.Q. Yu, S. Li, R.R. Shan, B. Du, Adsorption of acid dyes from aqueous solution by CTMAB modified bentonite: kinetic and isotherm modeling, J. Mol. Liq., 211 (2015) 1074–1081.
[4] Y. Bulut, H. Karaer, Adsorption of methylene blue from aqueous solution by crosslinked chitosan/bentonite composite, J. Dispersion Sci. Technol., 36 (2015) 61–67.
[5] Y. Liu, Y. Zheng, A. Wang, Enhanced adsorption of Methylene Blue from aqueous solution by chitosan-g-poly (acrylic acid)/vermiculite hydrogel composites, J. Environ. Sci., 22 (2010) 486–493.
[6] M. Foroughi-dahr, H. Abolghasemi, M. Esmaieli, G. Nazari, B. Rasem, Experimental study on the adsorptive behavior of Congo red in cationic surfactant-modified tea waste, Process Saf. Environ. Prot., 95 (2015) 226–236.
[7] R. Kamaraj, D. Davidson, G. Sozhan, S. Vasudevan, Adsorption of 2,4-dichlorophenoxyacetic acid (2,4-D) from water by in situ generated metal hydroxides using sacrificial anodes, J. Taiwan Inst. Chem. E., 45 (2014) 2943–2949.
[8] M. Ishaq, K. Saeed, I. Ahmad, S. Sultan, S. Akhtar, Coal ash as a low cost adsorbent for the removal of xylenol orange from aqueous solution, IJCCE, 33 (2014) 53–58.
[9] M. Fatiha, B. Belkacem, Adsorption of methylene blue from aqueous solutions using natural clay, J. Mater. Environ. Sci., 7 (2016) 285–292.
[10] R. Kamaraj, A. Pandiarajan, S. Jayakiruba, Mu. Naushad, S. Vasudevan, Kinetics, thermodynamics and isotherm modeling for removal of nitrate, J. Mol. Liq., 215 (2016) 204–211.
[11] M.J. Iqbal, M.N. Ashiq, Adsorption of dyes from aqueous solutions on activated charcoal, J. Hazard. Mater., 139 (2007) 57–66.
[12] A.R. Tehrani-Bagha, H. Nikkar, N.M. Mahmoodi, M. Markazi, F.M. Menger, The sorption of cationic dyes onto kaolin: Kinetic, isotherm and thermodynamic studies, Desalination, 266 (2011) 274–280.
[13] Q.H. Hu, S.Z. Qiao, F. Haghseresht, M.A. Wilson, G.Q. Lu, Adsorption study for removal of basic red dye using bentonite, Ind. Eng. Chem. Res., 45 (2006) 733–738.
[14] S. Wang, E. Ariyanto, Competitive adsorption of malachite green and Pb ions on natural zeolite, J. Colloid Interf. Sci., 314 (2007) 25–31.
[15] K.P. Jugal, R. Amutha, S. Radhe, P.K. Harminder, K. Akanksha, Adsorption of xylenol orange on Kigelia africana and Melia azedarach fruits based adsorbents from aqueous solution, IJACSA, 2 (2014) 1–7.
[16] C. Chen, M. Zhang, Q. Guan, W. Li, Kinetic and thermodynamic studies on the adsorption of xylenol orange onto MIL-101 (Cr), Chem. Eng. J., 183 (2012) 60–67.
[17] Y. Pontikes, G.N. Angelopoulos, Bauxite residue in cement and cementitious applications: current status and a possible way forward, Resour. Conserv. Recycl., 73 (2013) 53–63.

[18] Y. Ma, J. Zhu, H. He, P. Yuan, W. Shen, D. Liu, Infrared investigation of organo-montmorillonites prepared from different surfactants, Spectrochim. Acta, Part A, 76 (2010) 122–129.
[19] A. Dutta, N. Singh, Surfactant-modified bentonite clays: preparation, characterization, and atrazine removal, ESPR, 22 (2015) 3876–3885.
[20] M.A. Akl, A.M. Youssef, M.M. Al-Awadhi, Adsorption of acid dyes onto bentonite and surfactant-modified bentonite, J. Anal. Bioanal. Tech., 4 (2013) 3–7.
[21] M. Auta, B.H. Hameed, Modified mesoporous clay adsorbent for adsorption isotherm and kinetics of methylene blue, Chem. Eng. J., 198 (2012) 219–227.
[22] S. Tunali, A.S. Özcan, A. Özcan, T. Gedikbey, Kinetics and equilibrium studies for the adsorption of Acid Red 57 from aqueous solutions onto calcined-alunite, J. Hazard. Mater., 135 (2006) 141–148.
[23] Y.S. Al-Degs, M.I. El-Barghouthi, A.H. El-Sheikh, G.M. Walker, Effect of solution pH, ionic strength, and temperature on adsorption behavior of reactive dyes on activated carbon, Dyes Pigm., 77 (2008) 16–23.
[24] I. Langmuir, The adsorption of gases on plane surfaces of glass, mica and platinum, J. Am. Chem. Soc., 40 (1918) 1361–1403.
[25] H.M.F. Freundlich, Over the adsorption in solution, J. Phys. Chem., 57 (1906) 1100–1107.
[26] M.J. Temkin, V. Pyzhev, Recent modifications to Langmuir isotherms, Acta Phys-Chim. Sin., 12 (1940) 217–222.
[27] Mu. Naushada, S. Vasudevanb, G. Sharmac, A. Kumarc, Z.A. Al Othman, Adsorption kinetics, isotherms, and thermodynamic studies for Hg^{2+} adsorption from aqueous medium using alizarin red-S-loaded amberlite IRA-400 resin, Desal. Water Treat., 57 (2016) 1–9.
[28] S. Noreen, H.N. Bhatti, S. Nausheen, S. Sadaf, M. Ashfaq, Batch and fixed bed adsorption study for the removal of Drimarine Black CL-B dye from aqueous solution using a lignocellulosic waste: A cost affective adsorbent, Ind Crops Prod., 50 (2013) 568–579.
[29] M. Constantin, I. Asmarandei, V. Harabagiu, L. Ghimici, P. Ascenzi, G. Fundueanu, Removal of anionic dyes from aqueous solutions by an ion-exchanger based on pullulan microspheres, Carbohydr. Polym., 91 (2013) 74–84.
[30] M. Bouraada, M.S. Ouali, L.C. de Menorval, Dodecylsulfate and dodecybenzenesulfonate intercalated hydrotalcites as adsorbent materials for the removal of BBR acid dye from aqueous solutions, J. Saudi Chem. Soc., 20 (2016) 397–404.
[31] A.H. Jawad, R.A. Rashid, K. Ismail, S. Sabar, High surface area mesoporous activated carbon developed from coconut leaf by chemical activation with H_3PO_4 for adsorption of methylene blue, Desal. Wat. Treat., 74 (2017) 326–335.
[32] A. Tabak, N. Baltas, B. Afsin, M. Emirik, B. Caglar, E. Eren, Adsorption of Reactive Red 120 from aqueous solutions by cetylpyridinium-bentonite, J. Chem. Technol. Biotechnol., 85 (2010) 1199–1207.
[33] I.K. Georgiadis, A. Papadopoulos, N. Kantiranis, A. Filippidis, A. Tsirambides, sorption of Malachite green from aqueous solutions onto Greek raw diasporic bauxite, J. Environ. Prot. Ecol., 15 (2014) 606–615.
[34] E. Errais, J. Duplay, F. Darragi, I. M'Rabet, A. Aubert, F. Huber, G. Morvan, Efficient anionic dye adsorption on natural untreated clay: Kinetic study and thermodynamic parameters, Desalination, 275 (2011) 74–81.
[35] A.M. Aljeboree, A.F. Alkaim, A.H. Al-Dujaili, Adsorption isotherm, kinetic modeling and thermodynamics of crystal violet dye on coconut husk-based activated carbon, Desal. Water Treat., 53 (2015) 3656–3667.
[36] Z. Zhou, S. Lin, T. Yue, T.C. Lee, Adsorption of food dyes from aqueous solution by glutaraldehyde cross-linked magnetic chitosan nanoparticles, J. Food Eng., 126 (2014) 133–141.
[37] K. Kuśmierek, A. Świątkowski, Influence of Ph on adsorption kinetics of monochlorophenols from aqueous solutions on granular activated carbon, Ecol. Chem. Eng., 22 (2015) 95–105.
[38] M.M. Silva, M.M. Oliveira, M.C. Avelino, M.G. Fonseca, R.K. Almeida, E.C. Silva Filho, Adsorption of an industrial anionic dye by modified-KSF-montmorillonite: Evaluation of the kinetic, thermodynamic and equilibrium data, Chem. Eng. J., 203 (2012) 259–268.
[39] K.Y. Foo, B.H. Hameed, Insights into the modeling of adsorption isotherm systems, Chem. Eng. J., 156 (2010) 2–10.
[40] F. Shakeel, N. Haq, F.K. Alanazi, I.A. Alsarra, Removal of xylenol orange from its aqueous solution using SDS self-microemulsifying systems: optimization by Box–Behnken statistical design, Environ. Sci. Pollut. Res., 21 (2014) 5187–5200.
[41] O.S.A. Al-Khazrajy, A.B.A. Boxall, Impacts of compound properties and sediment characteristics on the sorption behaviour of pharmaceuticals in aquatic systems, J. Hazard. Mater., 317 (2016) 198–209.
[42] M. Kah, C.D. Brown, Adsorption of ionisable pesticides in soils, Rev. Environ. Contam. Toxicol., 188 (2006) 149–217.